Plant Biology ISSN 1435-8603

RESEARCH PAPER

Evidence for nickel/proton antiport activity at the tonoplast of the hyperaccumulator plant *Alyssum lesbiacum*

R. A. Ingle[1], M. D. Fricker[2] & J. A. C. Smith[2]

1 Department of Molecular and Cell Biology, University of Cape Town, Rondebosch, South Africa
2 Department of Plant Sciences, South Parks Road, Oxford, UK

Keywords
Alyssum; antiport; hyperaccumulator; nickel; tonoplast; vacuole.

Correspondence
R. A. Ingle, Department of Molecular and Cell Biology, University of Cape Town, Private Bag X3, Rondebosch 7701, South Africa.
E-mail: robert.ingle@uct.ac.za

Editor
G. Thiel

Received: 19 November 2007; Accepted: 23 January 2008

doi:10.1111/j.1438-8677.2008.00080.x

ABSTRACT

The mechanism of nickel uptake into vacuoles isolated from leaf tissue of *Alyssum lesbiacum* was investigated to help understand the ability of this species to hyperaccumulate Ni. An imaging system was designed to monitor Ni uptake by single vacuoles using the metal-sensitive fluorescent dye, Newport Green. Nickel uptake into isolated vacuoles from leaf tissue of *A. lesbiacum* was enhanced by the presence of Mg/ATP, presumably via energisation of the vacuolar H^+-ATPase (V-ATPase). This ATP-stimulated Ni uptake was abolished by bafilomycin (a diagnostic inhibitor of the V-ATPase) and by dissipation of the transmembrane pH difference with an uncoupler. These observations are consistent with Ni^{2+}/nH^+ antiport activity at the tonoplast driven by a proton electrochemical gradient established by the V-ATPase, which would provide a mechanism for secondary active transport of Ni^{2+} into the vacuole. This study provides insights into the molecular basis of Ni tolerance in *Alyssum*, and may aid in the identification of genes involved in Ni hyperaccumulation.

INTRODUCTION

Nickel hyperaccumulators form a group of taxonomically diverse plants that are defined by their remarkable ability to accumulate Ni to concentrations in excess of 0.1% shoot dry biomass (Baker & Brooks 1989; Reeves & Baker 2000). The genus *Alyssum* accounts for 48 of the 318 known Ni hyperaccumulator species, and includes *Alyssum lesbiacum* which is capable of accumulating Ni to over 3% shoot dry biomass (Baker *et al.* 2000; Reeves & Baker 2000). Ni accumulates predominantly in the aerial tissues of hyperaccumulators, although there is currently no consensus on the principal site of Ni storage in hyperaccumulators (Smart *et al.* 2007). At the tissue level, studies employing techniques such as X-ray microanalysis and high-resolution ion mass spectrometry have indicated that shoot epidermal cells are a major site of Ni deposition in hyperaccumulator plants, including several *Alyssum* species, *Cleome heratensis*, *Hybanthus floribundus* and *Senecio coronatus* (Mesjasz-Przybyłowicz *et al.* 1994; Küpper *et al.* 2001; Bidwell *et al.* 2004; Marquès *et al.* 2004; Asemaneh *et al.* 2006; de la Fuente *et al.* 2007). At the cellular level, there is also debate as to the respective roles played by the vacuole and apoplast in Ni sequestration. Whereas Krämer *et al.* (2000) estimated that approximately 70% of Ni in *Thlaspi goesingense* was associated with the apoplast, Küpper *et al.* (2001) reported that the majority of Ni was localised in the vacuoles in leaf tissue of *A. lesbiacum* and *T. goesingense*. This apparent discrepancy may be due in part to the different methods used to study Ni localisation (Smart *et al.* 2007).

The vacuole is the largest subcellular compartment, occupying 70–80% of the total volume of mature parenchymatous plant cells, and plays an important role in the storage of inorganic ions (Martinoia *et al.* 2007). It is rich in carboxylic acids, such as citric and malic acid, which may serve to chelate Ni with moderately high affinity (Saito *et al.* 2005; Smart *et al.* 2007). Furthermore, vacuolar storage of Ni has been implicated in Ni detoxification in yeast (Joho *et al.* 1992; Nishimura *et al.* 1998). If the vacuole is a site of Ni sequestration in hyperaccumulators, some form of active transport will be required at the tonoplast membrane to move Ni into the vacuole against its electrochemical gradient. The two possible mechanisms are primary active

transport, driven directly by the hydrolysis of ATP, or secondary active transport (*i.e.* Ni/proton antiport), in which ion movement would be coupled to the proton gradient generated by the vacuolar H^+ ATPase (V-ATPase) and vacuolar inorganic pyrophosphatase (V-PPase). Proton gradient-dependent Ni uptake at the tonoplast has previously been demonstrated in vacuolar membrane vesicles from yeast by the generation of an artificial proton gradient: collapse of the pH difference across the membrane, but not of the electrical potential difference, was found to abolish the uptake of Ni (Nishimura *et al.* 1998).

In this study, we developed a novel imaging method using a metal-sensitive fluorescent dye to investigate the mechanism of Ni uptake into vacuoles isolated from leaf tissue of the hyperaccumulator species, *Alyssum lesbiacum*. Ni uptake into the vacuole was measured as the change in fluorescence signal from isolated vacuoles loaded with the Ni-sensitive dye, Newport Green. Ni uptake was stimulated by Mg/ATP and was sensitive to known inhibitors of the V-ATPase and to abolition of the transmembrane proton gradient. Our results are consistent with the presence of an Ni^{2+}/H^+ antiport system at the tonoplast of *A. lesbiacum* that can drive vacuolar accumulation of Ni via a secondary active transport mechanism.

MATERIALS AND METHODS

Plant material and culture

Seeds of *Alyssum lesbiacum* (Candargy) Rech. f. (kindly provided by Prof. A. J. M. Baker) were germinated on moistened sand for 7 days, before being transferred to 1.2-l culture vessels and supplied with 1 l of modified 0.1 strength Hoagland solution, as previously described (Ingle *et al.* 2005b).

Fluorescent dyes

Newport Green DCF fluorescent dyes (dipotassium salt and diacetate), which incorporate di-(2-picolyl)amine chelator, were obtained from Molecular Probes (Invitrogen Ltd, Paisley, UK). Emission and excitation spectra of the dyes were characterised using a Perkin Elmer Luminescence Spectrometer (LS 50B) at 25 °C, with excitation and emission slit widths set at 2.5 nm. The maximum relative fluorescence yield for Newport Green DCF in the presence of various divalent cations at 100 μM is in the order: $Ni^{2+} > Co^{2+} > Zn^{2+} > Cd^{2+} > Fe^{2+}$ (Haugland 2002); the dye is insensitive to millimolar concentrations of Mg^{2+}(Dineley *et al.* 2002).

Protoplast isolation

Two grams of fresh leaf tissue were sliced into small pieces (approximately 1 mm^3), transferred to 50 ml of Wash Medium I (700 mM mannitol, 25 mM MES pH 5.7, KOH) and left for 15 min with occasional swirling. The wash medium was removed by pouring through muslin, and the pieces transferred to a Buchner filter where 12 ml of Isolation Medium (525 mM mannitol, 100 mM KCl, 50 mM MES (pH 5.7), 5 mM $MgSO_4$, 0.2% (w/v) polyvinylpyrrolidone-40, 1 mM DTT, 0.5% (w/v) bovine serum albumin, 1.35% (w/v) 'Onozuka' Cellulase RS (Yakult Honsha Co. Ltd, Tokyo, Japan), 0.075% (w/v) Pectolyase Y-23 (Seishin Pharmaceutical Co. Ltd, Tokyo, Japan)) were added and infiltrated under reduced pressure. The medium and pieces were then transferred to a flask and incubated for 70 min at room temperature. The extract was then centrifuged at $42 \times g$ for 5 min at 4 °C. The pellet was resuspended in 2 ml of loading buffer (700 mM mannitol, 25 mM MOPS (pH 7.5), 1 mM $MgSO_4$).

Dye loading

After resuspension of the pellet in loading buffer, the solution was shaken gently to encourage the cell plasmalemma to rupture. This mechanical disturbance was found to be sufficient to release isolated vacuoles. As treatments, 1 mM Mg/ATP, 200 nM bafilomycin A_1 or 2.5 mM ammonium sulphate were supplied to the samples immediately prior to dye loading. Dye loading was not affected by any of these treatments (data not shown). Newport Green DCF diacetate was added to a final concentration of 30 μM, followed by incubation for 1 h at room temperature to allow dye uptake and de-esterification.

Estimation of nickel uptake

After dye loading, 40 μl of the loading solution were transferred to a microscope sample chamber, which consisted of a 5-mm piece of the wide terminal end of a 200-μl pipette tip secured with Dow Corning 355 medical adhesive (Dow Corning Europe Inc., Brussels, Belgium) to a 22 mm × 40 mm coverslip. $NiSO_4$ was added to a final concentration of 100 μM. The chamber was placed on the microscope platform with a 22 mm × 22 mm coverslip covering the top of the chamber to prevent evaporation. A period of 15 min was allowed for the protoplasts and vacuoles to settle under gravity after the addition of Ni. During this time, the sample was illuminated with low-intensity white light to enable a suitable vacuole to be located, *i.e.* one that was spherical (suggesting that it was still viable), loaded with dye, and approximately 30 μm in diameter, which was mid-way in the size range of the vacuoles (10–40 μm). The selected vacuole was illuminated at 488 nm for 1 h, during which time the fluorescence emission at ≥520 nm from the area covered by the measurement aperture of the photometric system (30 μm × 30 μm) was recorded. The increase in fluorescence over the time course was used as a measure of Ni uptake by the vacuole.

Microscope and photometric system

The system used was a modified Nikon-Diaphot inverted epifluorescence microscope fitted with a 75-W xenon epifluorescence lamp. Light of ≥520 nm was allowed to pass from the sample to the microscope side port using a 510 nm dichroic mirror and a 520 nm long-pass emission filter. The microscope system was encased within a dark screen to minimise stray light interference. A standard Nikon variable aperture and PFX shutter system were attached to the emission side port of the fluorescence microscope. Light of ≥520 nm was detected by a 9924a photomultiplier (Thorn-EMI, Middlesex, UK). The photomultiplier signals were passed on to a single-photon counter (Newcastle Photonic Systems) configured to perform one count per second for 1 h.

Statistical analysis

All statistical tests were performed using MINITAB (version 12). The rate of increase in fluorescence intensity was approximately linear in all experiments, therefore, to reduce background noise, a linear regression was carried out on all data series. The regression equation obtained was used to calculate the fluorescence intensity of the area covered by the aperture at the start and end of each run, *i.e.* time 0 and 1 h. However, two other components also contributed to the fluorescence signal. First, the minor increase in signal from the medium surrounding the vacuole in the presence of Ni was measured and deducted from the count data. Second, continued dye loading into the vacuole over the course of the experiment also led to an increase in fluorescence signal over time. As determined in experiments in which no Ni was added to the loading buffer, the mean signal increase over 1 h from single vacuoles was 8.3 ± 0.3% (n = 5), so this value was also deducted from the count data. Percentage increase rather than absolute increase in signal was used to correct for differences in absolute signal intensity at the start of the experiment.

RESULTS

Ni accumulated in *Alyssum lesbiacum* vacuoles can be measured by Newport Green

To investigate whether the vacuole plays a role in Ni storage in *Alyssum lesbiacum*, a comparison of the fluorescence signal from protoplasts isolated from plants grown in solution culture in the presence of 0.3 mM Ni and plants not supplied with added Ni was carried out. Protoplasts from 2 g of fresh shoot tissue were isolated and the dipotassium salt form of Newport Green was added to a final concentration of 30 μM. The average number of protoplasts/vacuoles in the two isolates was calculated using a haemocytometer, and the volume adjusted to ensure that an equal number of protoplasts were included. No significant difference in emission at 529 nm was detected between the two protoplast preparations. However, addition of Triton X-100 to a final concentration of 0.03% (v/v) ruptured cell membranes and resulted in a fourfold higher signal from protoplasts isolated from plants grown in the presence of 0.3 mM Ni (data not shown). Calibration of the dye (Fig. 1) showed that the maximum response of the fully saturated dye was about sixfold higher than in the absence of Ni, with peak emission at 529 nm and an apparent K_d of 1.2 μM Ni^{2+}. This suggests that a fourfold increase in fluorescence following lysis corresponded to a final Ni concentration in the cuvette of just under 2 μM. Given that the estimated volume of protoplasts present initially was at least 1000-fold lower, these results would be consistent with mM concentrations of Ni in the protoplasts of plants exposed to Ni. As Ni is cytotoxic, the most likely intracellular site of accumulation would be the vacuole.

Mg/ATP enhances Ni uptake into isolated vacuoles

To determine the mechanism driving Ni accumulation into vacuoles of *A. lesbiacum*, we took advantage of the observed vacuolar accumulation of Newport Green when loaded into protoplasts as the membrane-permeant diacetate form (Fig. 2). The acetate groups are cleaved by esterases, resulting in intracellular accumulation of the membrane-impermeant free anion form of the dye. Vacuolar accumulation arises either directly from hydrolase action within the vacuole or following sequestration of any cytosolic dye released by the normal cytoplasmic detoxification pathways. Loaded vacuoles were released from the protoplasts by gentle mechanical agitation, and preliminary experiments demonstrated that it was possible to monitor the fluorescence signal from a single vacuole over a period of 1 h (data not shown).

To test whether Ni transport into the vacuole involved ATP-dependent active transport, the effect of Mg/ATP on Ni uptake was examined. Addition of 1 mM Mg/ATP to the loading buffer led to a significant increase in the average mean fluorescence signal change (Fig. 3) from 20.5 ± 2.8% h^{-1} in the absence of ATP to 34.0 ± 2.6% h^{-1} (P = 0.002, n = 11). We infer that Ni uptake into the vacuole occurred via an active transport mechanism energised by Mg/ATP.

Inhibition of V-ATPase activity abolishes Mg/ATP-stimulated Ni uptake

We next attempted to determine whether active transport of Ni into the vacuole was mediated via a primary transporter driven by hydrolysis of Mg/ATP, or via a secondary transporter energised by the proton electrochemical gradient. If Ni transport into the vacuole occurred via Ni^{2+}/H^{+}-antiport, it should be dependent on the proton electrochemical gradient established

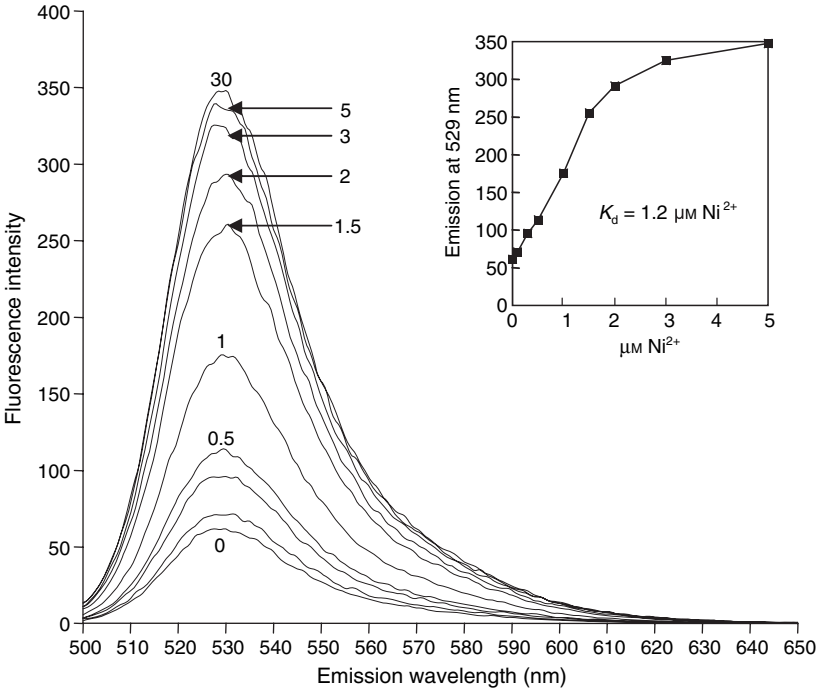

Fig. 1. Ni-dependent fluorescence emission spectra of Newport Green DCF (free anion form). Fluorescence emission was determined after excitation at 488 nm in the presence of 0–30 μM $NiSO_4$ in 5 mM MOPS (pH 7.0) at 25 °C. The Ni saturation curve for Newport Green is shown in the insert.

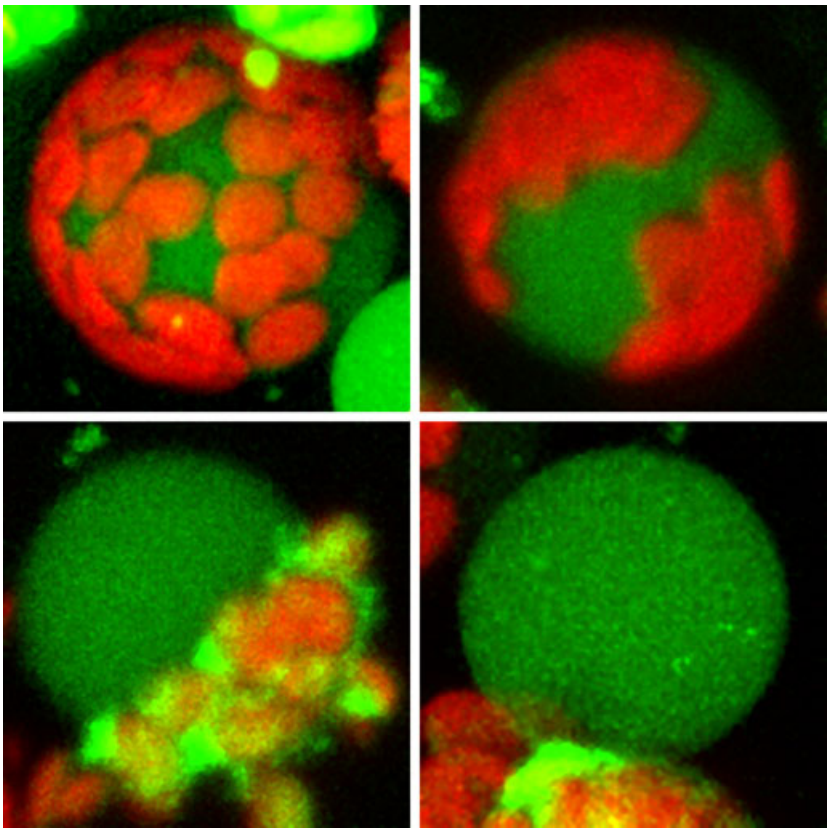

Fig. 2. Localisation of Newport Green dye to the vacuole. Protoplasts isolated from hydroponically cultivated plants exposed to 0.3 mM $NiSO_4$ were incubated with 30 μM Newport Green DCF (diacetate form) for 1 h. The fluorescence microscope images show the rupture of the plasma membrane and release of an intact vacuole loaded with Newport Green. The red signal is due to chlorophyll fluorescence in the chloroplasts. The protoplast was 30 μm in diameter. This figure is presented in colour online only.

across the tonoplast by the proton-pumping activities of the V-ATPase and V-PPase. Therefore, any disruption of this gradient should have a negative impact on Ni uptake. In contrast, if Ni were pumped into the vacuole via a primary transporter, such as a P-type ATPase or ATP-binding cassette (ABC) transporter,

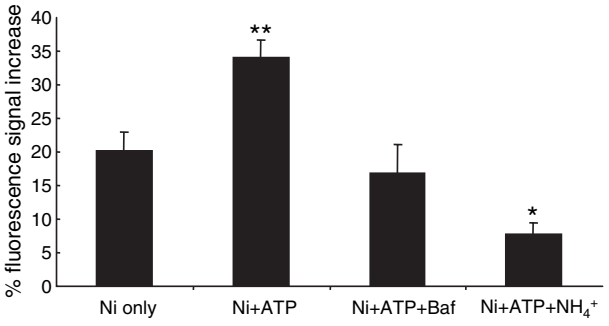

Fig. 3. Effect of Mg/ATP, bafilomycin and ammonium sulphate on Ni uptake. Ni uptake was measured as the percentage increase in fluorescence signal over 1 h from isolated vacuoles loaded with Newport Green DCF and exposed to 100 μM $NiSO_4$. Mean values ± SE are shown: Ni only (n = 11), Ni + ATP (n = 11), Ni + ATP + bafilomycin (n = 5) and Ni + ATP + ammonium sulphate (n = 5). Significant differences in fluorescence signal change compared with that observed in the presence of Ni only are indicated by *P < 0.05 and **P < 0.01.

Ni uptake and thus the increase in fluorescence signal should be unaffected by disruption of the proton electrochemical gradient.

Bafilomycin A_1, a macrolide antibiotic, is a highly specific inhibitor of the V-ATPase at concentrations <10 nmol·mg^{-1} protein (Bowman *et al.* 1988), preventing the formation of a proton electrochemical gradient across the tonoplast. The addition of 200 nM bafilomycin to the loading buffer completely abolished ATP-stimulated Ni uptake into the vacuole (Fig. 3); the mean fluorescence signal increase from vacuoles supplied with Mg/ATP and bafilomycin was not significantly different from those supplied with Ni only (P = 0.535, n = 5). The abolition of ATP-stimulated Ni uptake by bafilomycin suggested that it was indeed occurring via a secondary active transporter utilising the proton electrochemical gradient generated by the V-ATPase, rather than via a primary pump.

Uncoupling of the proton gradient abolishes Ni uptake

If dependent on the ΔpH component of the transmembrane proton electrochemical gradient, secondary active transport of Ni should be abolished by the addition of ammonium sulphate, as the NH_4^+/NH_3 couple rapidly dissipates the ΔpH across the tonoplast via equilibration of the weak base NH_3 (Barkla *et al.* 1995). The presence of 2.5 mM ammonium sulphate in the loading buffer again led to complete abolition of ATP-stimulated Ni uptake (Fig. 3). However, in contrast to bafilomycin-treated vacuoles, the increase in fluorescence signal from vacuoles exposed to ammonium sulphate was significantly lower than that from vacuoles supplied with Ni only in the absence of Mg/ATP at 7.7 ± 1.7% h^{-1} *versus* 20.3 ± 2.8% h^{-1} (P = 0.02, n = 5).

DISCUSSION

A system was designed to assay Ni uptake into isolated vacuoles from the hyperaccumulator plant *Alyssum lesbiacum* after loading with the highly Ni-sensitive dye Newport Green (Figs 1 and 2). The addition of Mg/ATP to the incubation medium led to a significant increase in Ni uptake, presumably via energisation of the V-ATPase, as this increase could be abolished by the highly specific V-ATPase inhibitor bafilomycin (Fig. 3). However, an increase in fluorescence signal over 1 h was observed from vacuoles even in the absence of Mg/ATP. We suggest this represents secondary active transport of Ni across the tonoplast of the intact vacuole utilising the pre-existing pH gradient between the incubation medium (pH 7.5) and the acidic interior of the vacuolar lumen. This is supported by the observation that collapse of the proton gradient by addition of an uncoupler (ammonium sulphate) all but abolished this signal increase (Fig. 3). The stimulation of Ni uptake by Mg/ATP and its dependence on the proton electrochemical gradient are consistent with the activity of an Ni^{2+}/H^+ antiport at the tonoplast of *A. lesbiacum*. While a pH gradient directed outwards from the vacuolar lumen would drive Ni^{2+} uptake by an H^+-antiport mechanism, the role of the electrical potential difference in this driving force would depend on the mechanistic stoichiometry of this transport system and cannot be established without further experimentation. As the epidermal cells are apparently a major site of Ni storage in *A. lesbiacum* (Küpper *et al.* 2001), future work could also aim to determine whether the Ni uptake mechanism identified here is more pronounced in epidermal cells compared to mesophyll cells (the likely source of vacuoles in the present study).

The ability to detect Ni^{2+} uptake driven by the transtonoplast proton electrochemical gradient is notable because other attempts to demonstrate Ni^{2+}/H^+ antiport across this membrane have been unsuccessful. For example, although evidence was found for H^+-linked antiport mechanisms for Zn, Mn and Cd uptake into tonoplast vesicles of oat (Gonzalez *et al.* 1999), no evidence could be found for energised uptake of Ni in this species (Gries & Wagner 1998). Using Newport Green, Saito *et al.* (2005) demonstrated sequestration of Ni in vacuoles of tobacco BY-2 suspension culture cells, but the mechanism of Ni transport was not studied directly. Similarly, Marquès *et al.* (2004) used Newport Green to detect Zn in the vacuole of the hyperaccumulator plant *Arabidopsis halleri*, but were not able to establish the mechanism of Zn transport in this species. Differences between species, and even between metal-tolerant and non-tolerant populations of the same species, are likely to be found in the predominant mechanism of vacuolar metal accumulation (Chardonnens *et al.* 1999).

The molecular identity of the putative Ni^{2+}/H^+ antiport system at the tonoplast is unknown. While a number of metal transport proteins whose transcripts are highly expressed in hyperaccumulator species have been identi-

fied, such as transporters of the *ZIP* gene family in the Zn/Cd hyperaccumulators *Thlaspi caerulescens* and *Arabidopsis halleri* (Pence *et al.* 2000; Assunção *et al.* 2001; Weber *et al.* 2004), and members of the cation diffusion facilitator family (Persans *et al.* 2001; Dräger *et al.* 2004), to date no Ni transporting protein has conclusively been identified at the tonoplast of a hyperaccumulator species. However, AtIREG2 was recently identified as a Ni transport protein in *Arabidopsis thaliana* (Schaaf *et al.* 2006). Heterologous expression of this protein complemented the Ni sensitivity of the yeast *cot1* mutant, but only at pH values below 5.0, suggesting that Ni transport is dependent on the proton electrochemical gradient. In *Arabidopsis*, the AtIREG2:GFP fusion protein was targeted to the tonoplast, and *35S:AtIREG2* lines displayed elevated tolerance to Ni, while T-DNA knock-outs displayed enhanced sensitivity (Schaaf *et al.* 2006). Interestingly, this Ni sensitivity was enhanced under conditions of Fe deficiency, which, coupled with the root-specific expression of *AtIREG2*, is suggestive of a role for this protein in proton gradient-dependent vacuolar loading of Ni in root tissue under Fe deficiency.

It is unclear whether the proton gradient-driven Ni uptake described in this study would occur via a specific Ni^{2+}/H^+ antiport, as cation/H^+ antiport proteins from plants sometimes display broad substrate specificity (Martinoia *et al.* 2007). For example, the Na^+/H^+ antiporter NHX1 can catalyse transport of K^+ into the vacuole (Venema *et al.* 2002), while members of the CAX family have broad substrate spectra (Shigaki & Hirschi 2006). It has been suggested that Ni can be transported via the same routes as Mg. For example, Ni uptake by *Saccharomyces cerevisiae* is competitively inhibited by Mg (Nishimura *et al.* 1998), while the bacterial CorA protein transports Mg and Ni (Smith *et al.* 1998), as does the *Arabidopsis* Mg transporter AtMGT (Li *et al.* 2001).

Whilst the transporters discussed above transport free ions, it is possible that Ni may be transported in a complex with a ligand. The tricarboxylic amino acid nicotianamine (NA) forms a complex with Ni in *T. caerulescens* (Vacchina *et al.* 2003), which can be transported by the yellow stripe-like transport protein TcYSL3 (Gendre *et al.* 2007). In *A. lesbiacum*, high concentrations of histidine in root tissue contribute to Ni tolerance in this species (Ingle *et al.* 2005a), and histidine has similarly been shown to chelate Ni *in vivo* (Krämer *et al.* 1996). Might Ni be transported into the vacuole as a Ni:His complex, possibly via an amino acid transporter? In the present study, addition of 100 μM histidine was not found to enhance Ni uptake into the vacuole (data not shown), and thus we have no evidence for such a transport mechanism in vacuolar sequestration of Ni. However, a role for an Ni:His transporter for xylem loading and unloading of Ni remains a strong possibility (Krämer *et al.* 1996; Kerkeb & Krämer 2003).

In conclusion, we have identified a mechanism by which Ni may be accumulated in the vacuoles of the Ni hyperaccumulator *Alyssum lesbiacum*. A major route of Ni uptake appears to be via secondary active transport (presumably by a Ni^{2+}/H^+-antiport mechanism), utilising the proton electrochemical gradient generated by the primary H^+ pump(s) at the tonoplast.

REFERENCES

Asemaneh T., Ghaderian S.M., Crawford S.A., Marshall A.T., Baker A.J.M. (2006) Cellular and subcellular compartmentation of Ni in the Eurasian serpentine plants *Alyssum bracteatum*, *Alyssum murale* (Brassicaceae) and *Cleome heratensis* (Capparaceae). *Planta*, **225**, 193–202.

Assunção A.G., DaCosta Martins P., De Folter S., Vooijs R., Schat H., Aarts M.G. (2001) Elevated expression of metal transporter genes in three accessions of the metal hyperaccumulator *Thlaspi caerulescens*. *Plant, Cell and Environment*, **24**, 217–226.

Baker A.J.M., Brooks R.R. (1989) Terrestrial higher plants which hyperaccumulate metallic elements – a review of their distribution, ecology and phytochemistry. *Biorecovery*, **1**, 81–126.

Baker A.J.M., McGrath S.P., Reeves R.D., Smith J.A.C. (2000) Metal hyperaccumulator plants: a review of the ecology and physiology of a biological resource for phytoremediation of metal-polluted soils. In: Terry N., Bañuelos G. (Eds), *Phytoremediation of contaminated soil and water*. Lewis Publishers, Boca Raton, FL: pp. 85–107.

Barkla B.J., Zingarelli L., Blumwald E., Smith J.A.C. (1995) Tonoplast Na^+/H^+ antiport activity and its energization by the vacuolar H^+-ATPase in the halophytic plant *Mesembryanthemum crystallinum* L. *Plant Physiology*, **109**, 549–556.

Bidwell S.D., Crawford S.A., Woodrow I.E., Sommer-Knudsen J., Marshall A.T. (2004) Sub-cellular localization of Ni in the hyperaccumulator, *Hybanthus floribundus* (Lindley) F. Muell. *Plant, Cell and Environment*, **27**, 705–716.

Bowman E.J., Siebers A., Altendorf K. (1988) Bafilomycins: A class of inhibitors of membrane ATPases from microorganisms, animal cells, and plant cells. *Proceedings of the National Academy of Sciences USA*, **85**, 7972–7976.

Chardonnens A.N., Koevoets P.L.M., van Zanten A., Schat H., Verkleij J.A.C. (1999) Properties of enhanced tonoplast zinc transport in naturally selected zinc-tolerant *Silene vulgaris*. *Plant Physiology*, **120**, 779–785.

Dineley K.E., Malaiyandi L.M., Reynolds I.J. (2002) A re-evaluation of neuronal zinc measurements: artifacts associated with high intracellular dye concentration. *Molecular Pharmacology*, **62**, 618–627.

Dräger D.B., Desbrosses-Fonrouge A., Krach C., Chardonnens A.N., Meyer R.C., Saumitou-Laprade P., Krämer U. (2004) Two genes encoding *Arabidopsis halleri* MTP1 metal transport proteins co-segregate with zinc tolerance and account for high *MTP1* transcript levels. *The Plant Journal*, **39**, 425–439.

de la Fuente V., Rodriguez N., Diez-Garretas B., Rufo L., Asensi A., Amils R. (2007) Nickel distribution in the hyperaccumulator *Alyssum serpyllifolium* Desf. spp. from the Iberian Peninsula. *Plant Biosystems*, **141**, 170–180.

Gendre D., Czernic P., Conéjéro G., Pianelli K., Briat J.-F., Lebrun M., Mari S. (2007) *TcYSL3*, a member of the YSL gene family from the hyper-accumulator *Thlaspi caerulescens*, encodes a nicotianamine-Ni/Fe transporter. *The Plant Journal*, **49**, 1–15.

Gonzalez A., Koren'kov V., Wagner G.J. (1999) A comparison of Zn, Mn, Cd, and Ca transport mechanisms in oat root transport vesicles. *Physiologia Plantarum*, **106**, 203–209.

Gries G.E., Wagner G.J. (1998) Association of nickel versus transport of cadmium and calcium in tonoplast vesicles of oat roots. *Planta*, **204**, 390–396.

Haugland R.P. (2002) *Handbook of Fluorescent Probes and Research Products*, 9th edn. Molecular Probes, Inc., Eugene, OR.

Ingle R.A., Mugford S.T., Rees J.D., Campbell M.M., Smith J.A.C. (2005a) Constitutively high expression of the histidine biosynthetic pathway contributes to nickel tolerance in hyperaccumulator plants. *Plant Cell*, **17**, 2089–2106.

Ingle R.A., Smith J.A.C., Sweetlove L.J. (2005b) Responses to nickel in the proteome of the hyperaccumulator plant *Alyssum lesbiacum*. *BioMetals*, **18**, 627–641.

Joho M., Ishikawa Y., Kunikane M., Inouhe M., Tohoyama H., Murayama T. (1992) The subcellular-distribution of nickel in Ni-sensitive and Ni-resistant strains of *Saccharomyces cerevisiae*. *Microbios*, **71**, 149–159.

Kerkeb L., Krämer U. (2003) The role of free histidine in xylem loading of nickel in *Alyssum lesbiacum* and *Brassica juncea*. *Plant Physiology*, **131**, 716–724.

Krämer U., Cotter-Howells J.D., Charnock J.M., Baker A.J.M., Smith J.A.C. (1996) Free histidine as a metal chelator in plants that accumulate nickel. *Nature*, **379**, 635–638.

Krämer U., Pickering I.J., Prince R.C., Raskin I., Salt D.E. (2000) Subcellular localization and speciation of nickel in hyperaccumulator and non-accumulator *Thlaspi* species. *Plant Physiology*, **122**, 1343–1353.

Küpper H., Lombi E., Zhao F.J., Wieshammer G., McGrath S.P. (2001) Cellular compartmentation of nickel in the hyperaccumulators *Alyssum lesbiacum*, *Alyssum bertolonii* and *Thlaspi goesingense*. *Journal of Experimental Botany*, **52**, 2291–2300.

Li L., Tutone A.F., Drummond R.S.M., Gardner R.C., Luan S. (2001) A novel family of magnesium transport genes in *Arabidopsis*. *Plant Cell*, **13**, 2761–2775.

Marquès L., Cossegal M., Bodin S., Czernic P., Lebrun M. (2004) Heavy metal specificity of cellular tolerance in two hyperaccumulating plants, *Arabidopsis halleri* and *Thlaspi caerulescens*. *New Phytologist*, **164**, 289–295.

Martinoia E., Maeshima M., Neuhaus H.E. (2007) Vacuolar transporters and their essential role in plant metabolism. *Journal of Experimental Botany*, **58**, 83–102.

Mesjasz-Przybyłowicz J., Balkwill K., Przybyłowicz W.J., Annegarn H.J. (1994) Proton microprobe and X-ray fluorescence investigations of nickel distribution in serpentine flora from South Africa. *Nuclear Instruments and Methods in Physics Research B*, **89**, 208–212.

Nishimura K., Igarashi K., Kakinuma Y. (1998) Proton gradient-driven nickel uptake by vacuolar membrane vesicles of *Saccharomyces cerevisiae*. *Journal of Bacteriology*, **180**, 1962–1964.

Pence N.S., Larsen P.B., Ebbs S.D., Letham D.L., Lasat M.M., Garvin D.F., Eide D., Kochian L.V. (2000) The molecular physiology of heavy metal transport in the Zn/Cd hyperaccumulator *Thlaspi caerulescens*. *Proceedings of the National Academy of Sciences USA*, **97**, 4956–4960.

Persans M.W., Nieman K., Salt D.E. (2001) Functional activity and role of cation-efflux family members in Ni hyperaccumulation in *Thlaspi goesingense*. *Proceedings of the National Academy of Sciences USA*, **98**, 9995–10000.

Reeves R.D., Baker A.J.M. (2000) Metal-accumulating plants. In: Raskin I., Ensley B.D. (Eds), *Phytoremediation of Toxic Metals: Using Plants to Clean Up the Environment*. Wiley and sons, New York: pp. 193–229.

Saito A., Higuchi K., Hirai M., Nakane R., Yoshiba M., Tadano T. (2005) Selection and characterization of a nickel-tolerant cell line from tobacco (*Nicotiana tabacum* cv. bright yellow-2) suspension culture. *Physiologia Plantarum*, **125**, 441–453.

Schaaf G., Honsbein A., Meda A.R., Kirchner S., Wipf D., von Wirén N. (2006) *AtIREG2* encodes a tonoplast transport protein involved in iron-dependent nickel detoxification in *Arabidopsis thaliana* roots. *Journal of Biological Chemistry*, **281**, 25532–25540.

Shigaki T., Hirschi K.D. (2006) Diverse functions and molecular properties emerging for CAX cation/H^+ exchangers in plants. *Plant Biology*, **8**, 419–429.

Smart K.E., Kilburn M.R., Salter C.J., Smith J.A.C., Grovenor C.R.M. (2007) NanoSIMS and EPMA analysis of nickel localisation in leaves of the hyperaccumulator plant *Alyssum lesbiacum*. *International Journal of Mass Spectrometry*, **260**, 107–114.

Smith R.L., Szegedy M.A., Kucharski L.M., Walker C., Wiet R.M., Redpath A., Kaczmarek M.T., Maguire M.E. (1998) The CorA Mg^{2+} transport protein of *Salmonella typhimurium*. Mutagenesis of conserved residues in the third membrane domain identifies a Mg^{2+} pore. *Journal of Biological Chemistry*, **273**, 28663–28669.

Vacchina V., Mari S., Czernic P., Marquès L., Pianelli K., Schaumlöffel D., Lebrun M., Łobiński R. (2003) Speciation of nickel in a hyperaccumulating plant by high-performance liquid chromatography–inductively coupled plasma mass spectrometry and electrospray MS/MS assisted by cloning using yeast complementation. *Analytical Chemistry*, **75**, 2740–2745.

Venema K., Quintero F.J., Pardo J.M., Donaire J.P. (2002) The *Arabidopsis* Na^+/H^+ exchanger AtNHX1 catalyzes low

affinity Na^+ and K^+ transport in reconstituted liposomes. *Journal of Biological Chemistry*, **277**, 2413–2418.

Weber H., Harada E., Vess C., Roepenack-Lahaye E., Clemens S. (2004) Comparative microarray analysis of *Arabidopsis thaliana* and *Arabidopsis halleri* roots identifies nicotianamine synthase, a ZIP transporter and other genes as potential metal hyperaccumulation factors. *The Plant Journal*, **37**, 269–281.